

Functional significance of Glu-77 and Tyr-137 within the active site of isoaspartyl dipeptidase

Ricardo Martí-Arbona^b, James B. Thoden^a,
Hazel M. Holden^a, Frank M. Raushel^{b,*}

^a Department of Biochemistry, University of Wisconsin, Madison, WI 53706, USA

^b Department of Chemistry, PO Box 30012, Texas A&M University, College Station, TX 77842-3012, USA

Received 19 August 2005

Available online 11 November 2005

Abstract

Isoaspartyl dipeptidase (IAD) is a binuclear metalloenzyme and a member of the amidohydrolase superfamily. This enzyme catalyzes the hydrolytic cleavage of β -aspartyl dipeptides. The pH-rate profiles for the hydrolysis of β -Asp-Leu indicates that catalysis is dependent on the ionization of two groups; one that ionizes at a pH \sim 6 and the other \sim 9. The group that must be ionized for catalysis is directly dependent on the identity of the metal ion bound to the active site. This result is consistent with the ionization of the hydroxide that bridges the two divalent cations. In addition to the residues that interact directly with the divalent cations there are two other residues that are highly conserved and found within the active site: Glu-77 and Tyr-137. Mutation of Tyr-137 to phenylalanine reduced the rate of catalysis by three orders of magnitude. The three dimensional X-ray structure of the Y137F mutant did not show any significant conformation changes relative to the three dimensional structure of the wild-type enzyme. The positioning of the side-chain phenolic group of Tyr-137 in the active site of IAD is consistent with the stabilization of the tetrahedral adduct concomitant with nucleophilic attack by the hydroxide that bridges the two divalent cations. Mutation of Glu-77 resulted in the reduction of catalytic activity by five orders of magnitude. The three dimensional structure of the E77Q mutant did not show any significant conformational changes in the mutant relative to the three dimensional structure of the wild-type enzyme. The positioning of the side-chain carboxylate of Glu-77 is consistent with the formation of an ion pair interaction with the free α -amino group of the substrate. © 2005 Elsevier Inc. All rights reserved.

Keywords: Isoaspartyl dipeptidase

* Corresponding author. Fax: +1 979 845 9452.

E-mail address: raushel@tamu.edu (F.M. Raushel).

1. Introduction

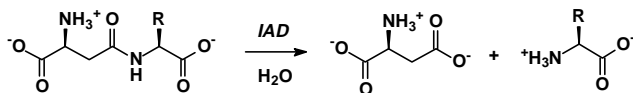
Isoaspartyl dipeptidase (IAD)¹ catalyzes the hydrolytic cleavage of β -aspartyl dipeptides [1–3]. These unusual peptide bonds are formed via the spontaneous, but slow, isomerization of the protein backbone at amide bonds to asparagine and aspartate residues. The best substrate found to date for this enzyme is β -Asp-Leu with a K_m of 1.0 mM and a k_{cat} of 104 s^{-1} [4]. However, IAD exhibits no activity toward the hydrolysis of tripeptides or γ -glutamyl dipeptides [1,2]. Amino acid sequence identity and three dimensional structure comparisons demonstrate that this enzyme is a member of the amidohydrolase superfamily and most closely resembles dihydroorotase and D-hydantoinase [5,6]. The general reaction catalyzed by IAD is presented in Scheme 1.

Three dimensional crystal structures of IAD have been solved to high resolution [4,7,8]. These structures include the apo-enzyme and complexes with the substrate (β -Asp-His), product (aspartate), and a phosphonate inhibitor [4,6]. The individual subunits of the octameric protein are folded into two domains. The N-terminal domain is composed of eight mixed β -strands while the C-terminal domain folds as a conventional $(\beta/\alpha)_8$ -barrel. A binuclear metal center is located within the active site at the C-terminal end of the $(\beta/\alpha)_8$ -barrel motif. The two metal ions are ligated by four histidines, an aspartic acid and a carboxylated lysine residue. The α -metal ion is coordinated by His-68, His-70, and Asp-285 while the β -metal is coordinated by His-201 and His-230. The two metal ions are bridged by the carboxylated Lys-162 and a molecule from solvent that is presumed to be hydroxide.

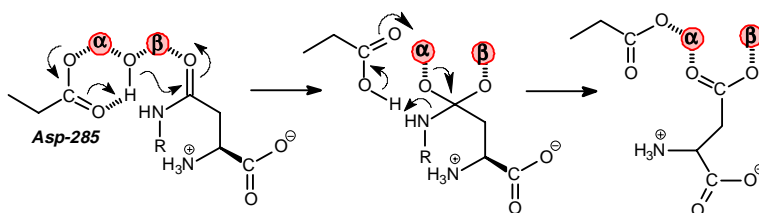
Kinetic and structural investigations of IAD have indicated that the binuclear metal center is critical for the enhancement of the nucleophilic character of the hydrolytic water molecule and the activation of the peptide bond prior to substrate turnover. The β -metal ion is thought to polarize the carbonyl oxygen bond while the α -metal ion has been proposed to stabilize the binding of hydroxide [4,8]. The side-chain carboxylate group of Asp-285 has been postulated to shuttle the proton from the bridging hydroxide to the α -amino group of the departing amino acid during cleavage of the peptide bond [4,8]. Support for this chemical mechanism is derived from the X-ray crystal structures of the wild-type and D285N mutant enzymes and the pH-rate profiles of the wild-type enzyme substituted with a variety of divalent cations [4]. The proposed reaction mechanism is presented in Scheme 2.

The pH-rate profile of wild-type IAD displays a bell-shaped dependence for the hydrolysis of β -Asp-Leu [4]. The decrease in catalytic activity at low pH indicates that the protonation of a single group results in the loss of catalytic activity. The systematic variation in the kinetic pK_a , obtained from the pH-rate profiles with different metal substituted variants of IAD, demonstrated that the pK_a for the ionization at low pH is dependent on the identity of metal ions in the binuclear metal center [4]. This result is consistent with the protonation of the bridging hydroxide. The pK_a of the group that needs to be protonated for catalytic activity is independent of changes to the specific metal ion bound within the binuclear metal center. This ionization has been proposed to be due to deprotonation of the α -amino group of the aspartate moiety of the substrate [4].

¹ Abbreviations used: DHO, dihydroorotase; IAD, isoaspartyl dipeptidase; Hepes, *N*-2-hydroxyethylpiperazine-*N'*-2-ethanesulfonic acid; Ches, 2-(cyclohexylamino)ethanesulfonic acid; Mes, 2-morpholinoethanesulfonic acid; Pipes, piperazine-*N,N'*-bis(2-ethanesulfonic acid); Taps, *N*-[Tris-(hydroxymethyl)methyl]-3-aminopropanesulfonic acid.



Scheme 1.



Scheme 2.

In addition to the residues that make direct interactions with the binuclear metal center in the active site of IAD, there are two other highly conserved residues within the active site that may contribute to the overall rate enhancement for this enzyme. In the X-ray crystal structure of IAD, the side-chain phenolic group of Tyr-137 is orientated in a position where it may function as a 5th metal ligand to the β -metal ion and/or serve as a Lewis acid catalyst for the polarization of the carbonyl oxygen of the scissile amide bond. The side chain carboxylate of Glu-77 likely functions in an ion pair arrangement with the free α -amino group of the substrate or, alternatively, as part of a proton shuttle mechanism.

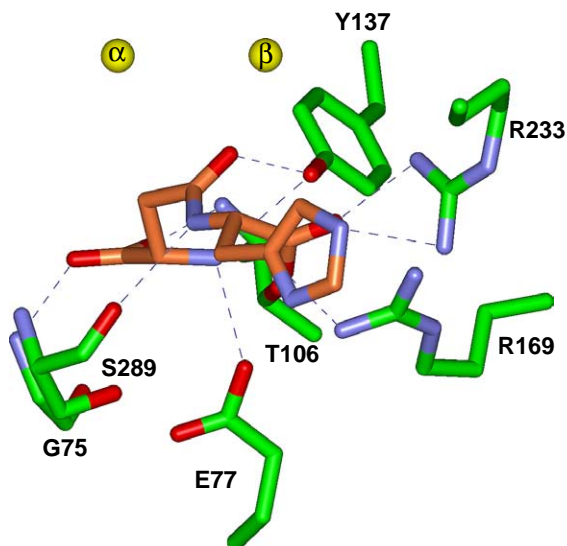


Fig. 1. A close-up view of the active site of the D285N mutant with bound β -Asp-His, highlighted in gold bonds. Potential hydrogen bonding interactions between β -Asp-His and the D285N mutant are represented by the blue dashed lines. The side-chain phenolic oxygen of Y137 is 2.4 Å away from the carbonyl oxygen of the scissile bond of the bound substrate. The side-chain carboxylate of E77 is 2.9 Å away from the free α -amino group of the bound β -Asp-His. The image was drawn with the program WebLab Viewer Pro using the coordinates from PDB file 1YBQ (4).

The relative orientations of these two residues within the active site of IAD are presented in Fig. 1. In this article, we have probed the contribution of these two residues in the catalytic activity of IAD by measuring the kinetic constants for site directed mutants of IAD and have determined the alterations in the three dimensional structure by electron diffraction for E77Q and Y137F.

2. Materials and methods

2.1. Materials

All chemicals, substrates, and coupling enzymes were obtained from Sigma or Aldrich. The *iadA* gene was cloned from the *Escherichia coli* XL1Blue strain into a pET30 plasmid obtained from Stratagene [8]. Site directed mutagenesis of IAD at residues Glu-77 and Tyr-137 was accomplished using the Quick Change site-directed mutagenesis kit from Stratagene.

2.2. Protein purification

The pET30 plasmids encoding wild-type and mutant IAD were transformed in JDG 1000 (λ DE3). IAD was purified according to published procedures [4]. Cultures were grown in Luria–Bertani medium at 37 °C until the absorbance at 600 nm reached 0.6 OD. The expression of IAD was induced by the addition of 1.0 mM isopropyl- β -thiogalactoside and incubated for 12 h at 37 °C. Cells were harvested by centrifugation and resuspended in 50 mM Hepes buffer at pH 8.1 (buffer A) containing 5 μ g/mL RNase and 0.1 mg/mL phenylmethylsulfonyl fluoride. The cells were lysed by sonication and the soluble protein was isolated by centrifugation and then fractioned between 20 and 50% saturation of ammonium sulfate in buffer A. The precipitated protein was resuspended and loaded onto a Superdex 200 gel filtration column (Amersham Pharmacia). The active fractions were pooled and loaded onto a Resource Q ionic exchange column (Amersham Pharmacia) and eluted with a gradient of NaCl in buffer A. The purification was finalized by pooling and precipitating the fractions that contained IAD with ammonium sulfate. The pellet was resuspended and reloaded onto the Superdex 200 gel filtration column and eluted with buffer A. The presence and purity of IAD in the fractions was confirmed by SDS–PAGE. The chromatographic profiles for wild-type and mutant IAD were identical. The purified enzyme was stored at –20 °C.

2.3. Kinetic measurements and data analysis

The specific activity of IAD was assayed by the coupling the formation of aspartate to the oxidation of NADH [9]. The oxidation of NADH at 30 °C was followed spectrophotometrically at 340 nm with a SPECTRAmax-340 microplate reader (Molecular Devices Inc.). The assay solutions contained 100 mM Hepes, 100 mM KCl, 3.7 mM α -ketoglutarate, 0.4 mM NADH, and 0.64 U of malate dehydrogenase, 6 U of aspartate aminotransferase, and variable amounts of β -Asp-Leu and IAD in a final volume of 250 μ L. The kinetic constants were determined by fitting the initial velocity data to the Eq. (1) [10]. In Eq. (1), v is the initial velocity, E_t is the enzyme concentration, k_{cat} is the turnover number, A is the substrate concentration, and K_m is the Michaelis constant.

The pH dependence of the kinetic parameters was determined for the Zn/Zn-substituted forms of the wild-type and the Y135F mutant using β -Asp-Leu as the variable substrate. The pH range was assayed between 5.0 and 10.0 in 0.2 pH unit increments. The buffers Mes (5.0–6.6), Pipes (6.6–7.2), Hepes (7.2–8.2), Taps (8.2–8.8), and Ches (8.8–10.0) were used at a concentration of 100 mM and the pH of each solution was measured after the reaction was completed. Eq. (2) was utilized to fit the data when the activity diminished at both low and high pH [10]. In Eq. (2), y is the value of k_{cat} or k_{cat}/K_m , c is the pH-independent value of y , K_a and K_b are the dissociation constants of the groups that ionize and H is the hydrogen-ion concentration.

$$v/E_t = k_{\text{cat}}A/(K_m + A) \quad (1)$$

$$\log y = \log(c/(1 + (H/K_a) + (K_b/H))) \quad (2)$$

2.4. Structural analysis

Large single crystals of the E77Q and Y137F mutant proteins were grown by the hanging drop method of vapor diffusion against precipitant solutions containing 6–8%

Table 1
X-ray data collection statistics

| Data set | Resolution (Å) | Independent reflections | Completeness (%) | Redundancy | Avg I /Avg σ (I) | R_{sym} ^a |
|----------|------------------------|-------------------------|------------------|------------|-------------------------------|-------------------------------|
| E77Q | 30.0–1.95 | 68348 | 93.4 | 3.7 | 8.2 | 7.0 |
| | 2.04–1.95 ^b | 6900 | 75.7 | 1.5 | 1.7 | 28.0 |
| Y137F | 30.0–1.95 | 71537 | 97.9 | 3.3 | 11.6 | 6.5 |
| | 2.04–1.95 | 7448 | 81.8 | 1.8 | 2.5 | 26.4 |

^a $R_{\text{sym}} = \sum |I - \bar{I}| / \sum I \times 100$.

^b Statistics for the highest resolution bin.

Table 2
Relevant refinement statistics

| Complex | E77Q | Y149F |
|---|-------------------|-------------------|
| Resolution limits (Å) | 30.0–1.95 | 30.0–1.95 |
| ^a R -factor (overall)%/# rflns | 18.0/68348 | 18.5/71537 |
| R -factor (working)%/# rflns | 17.9/61482 | 18.3/64418 |
| R -factor (free)%/# rflns | 21.9/6866 | 21.3/7119 |
| No. Protein atoms | 5579 ^b | 5559 ^c |
| No. Hetero-atoms | 426 ^d | 375 ^e |
| Bond lengths (Å) | 0.013 | 0.013 |
| Bond angles (°) | 2.29 | 2.33 |
| Trigonal planes (Å) | 0.008 | 0.009 |
| General planes (Å) | 0.016 | 0.014 |
| Torsional angles (°) ^f | 16.9 | 16.3 |

^a R – factor = $(\sum |F_o - F_c|) / \sum |F_o| \times 100$ where F_o is the observed structure-factor amplitude and F_c is the calculated structure-factor amplitude.

^b These include multiple conformations for V100 and N341 in chain A and K150 and N341 in chain B.

^c These include multiple conformations for V100, R330, and N341 in chain A and V100 and N341 in chain B.

^d These include 4 zinc ions and 422 waters.

^e These include 4 zinc ions and 371 waters.

^f The torsional angles were not restrained during the refinement.

poly(ethylene glycol) 8000, 100 mM homopipes (pH 5.0), and 50–100 mM MgCl_2 . They contained two subunits in the asymmetric unit and belonged to space group $P4_212$ with unit cell dimensions of $a = b = 119.2 \text{ \AA}$ and $c = 138.6 \text{ \AA}$. X-ray data sets were collected to 1.95 Å resolution at 4 °C with a Bruker HISTAR area detector system equipped with Supper “long” mirrors. The X-ray source was Cu $K\alpha$ radiation from a Rigaku RU200 X-ray generator operated at 50 kV and 90 mA. The X-ray data were processed with XDS [11,12] and internally scaled with XSCALIBRE (Rayment and Wesenberg, unpublished program). Relevant X-ray data collection statistics are presented in Table 1.

The structure was determined by difference Fourier techniques using as a starting model the wild-type structure (PDB 1ONW). Iterative cycles of least-squares refinement with TNT [13] and manual model building reduced the R -factors to 18.0% (for the E77Q) and 18.5% (for the Y137F) all measured X-ray data from 30.0 to 1.95 Å resolution. Relevant least-squares refinement statistics are given in Table 2.

3. Results

3.1. Mutation of residues glutamate-77 and tyrosine-137

The kinetic parameters for the Zn/Zn-substituted forms of the wild-type and mutants of IAD at pH 8.1 are presented in Table 3. Wild-type IAD exhibits a K_m of 1.0 mM and a k_{cat}/K_m of $10^5 \text{ M}^{-1} \text{ s}^{-1}$ for the catalytic hydrolysis of β -Asp-Leu [4]. The mutation of Glu-77 to either alanine or aspartate results in a significant decrease in the specific activity by reducing the k_{cat} by approximately five orders of magnitude. For the mutant E77D, the K_m is increased 7-fold but there is no apparent effect on the K_m for the E77Q mutant. Site directed mutagenesis of Tyr-137 to an alanine resulted in a mutant with a K_m that is elevated by 2.5-fold relative to the wild-type enzyme. The K_m for the phenylalanine mutant at this site is identical to the wild-type enzyme. For both mutants made at position Y137 the value of k_{cat} is diminished by about three orders of magnitude.

3.2. pH-rate profiles

The kinetic $\text{p}K_a$ values were determined from the pH-dependence of the catalytic parameters for wild-type IAD and the Y137F mutant. The pH-rate profiles for wild-type IAD and the Y137F mutant are bell-shaped as presented in Fig. 2. These results indicate that one group must be unprotonated while another group must be protonated for opti-

Table 3
Kinetic parameters for IAD and mutants with β -Asp-Leu as the substrate^a

| IAD | K_m (mM) | k_{cat} (s^{-1}) | k_{cat}/K_m ($\text{M}^{-1}\text{s}^{-1}$) |
|-------|-----------------|--------------------------------------|---|
| WT | 1.0 ± 0.1 | $(1.04 \pm 0.03) \times 10^2$ | $(1.0 \pm 0.1) \times 10^5$ |
| E77D | 6.9 ± 0.9 | $(5.1 \pm 0.3) \times 10^{-3}$ | $(7.4 \pm 0.1) \times 10^{-1}$ |
| E77Q | 0.8 ± 0.1 | $(5.6 \pm 0.1) \times 10^{-3}$ | 7 ± 1 |
| Y137A | 2.5 ± 0.2 | $(3.2 \pm 0.1) \times 10^{-1}$ | $(1.26 \pm 0.01) \times 10^1$ |
| Y137F | 0.97 ± 0.07 | $(3.1 \pm 0.1) \times 10^{-1}$ | $(3.16 \pm 0.1) \times 10^1$ |

^a The kinetic constants were determined at pH 8.1 from a fit of the data to Eq. (1).

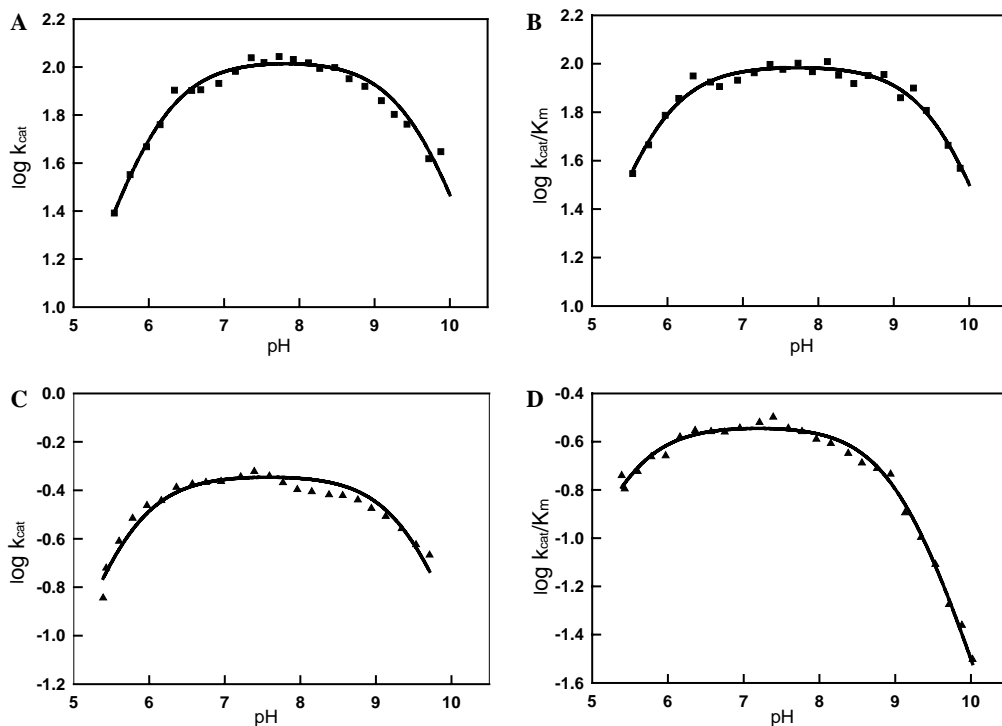


Fig. 2. The pH-rate profiles of k_{cat} and k_{cat}/K_m for wild-type (■), and Y137F mutant enzyme (▲). The pH-rate profiles for the wild-type enzyme are presented in (A and B). The pH-rate profiles for the mutant Y137F are shown in (C and D). The data were fit to Eq. (2) using β -Asp-Leu as the variable substrate. Additional details are provided in the text and in Table 4.

imum catalytic activity. The $\text{p}K_a$ values for wild-type IAD and the Y137F mutant, obtained from fits of the data to Eq. (2), are provided in Table 4. For the mutant Y137F, the $\text{p}K_a$ value for the group that must be unprotonated for maximum catalytic activity, obtained from the variation of k_{cat} with pH, is somewhat lower than the value observed with the wild-type enzyme (5.6 relative to 6.1 for wild-type IAD). The $\text{p}K_a$ for the group that must be protonated for maximum catalytic activity is essentially the same for the mutant and the wild-type enzyme. A bell-shaped profile was also observed for the wild-type IAD when k_{cat}/K_m was measured as function of pH. For the mutant enzyme, the kinetic $\text{p}K_a$ values for the two ionizations from k_{cat}/K_m are somewhat lower than that observed for the wild-type enzyme.

Table 4
 $\text{p}K_a$ values for wild-type and Y137F mutant of IAD from pH-rate profiles^a

| IAD | log k_{cat} vs. pH | | log k_{cat}/K_m vs. pH | |
|-------|-----------------------------|---------------|---------------------------------|---------------|
| | $\text{p}K_a$ | $\text{p}K_b$ | $\text{p}K_a$ | $\text{p}K_b$ |
| WT | 6.1 ± 0.4 | 9.6 ± 0.1 | 5.8 ± 0.4 | 9.6 ± 0.1 |
| Y137F | 5.6 ± 0.1 | 9.6 ± 0.1 | 5.3 ± 0.1 | 9.1 ± 0.1 |

^a The kinetic constants were determined with β -Asp-Leu as the substrate from a fit of the data to Eq. (2).

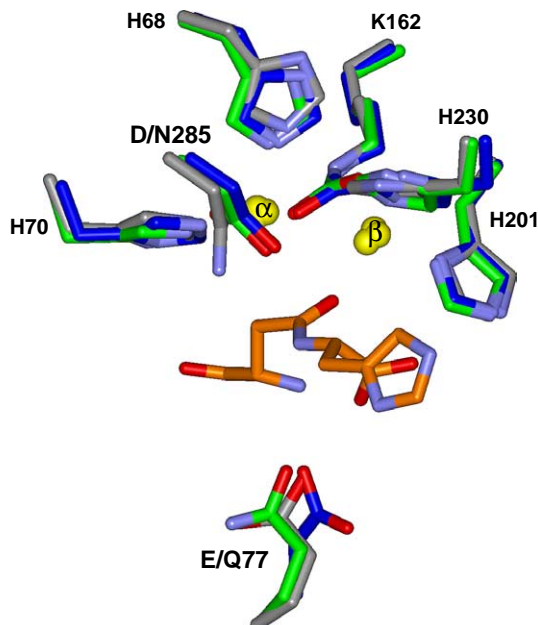


Fig. 3. Superposition of the active site region for the apo-form of IAD (PDB: 1ONW), the mutant E77Q (PDB: 2AQO), and the substrate bound complex of the mutant D285N (PDB: 1YBQ). The side chains of the apo-form of IAD are depicted with blue bonds, the side chains for the E77Q mutant are depicted in green, and the substrate bound complex of the D285N mutant is displayed in grey. The positions of the zinc ions for all of the structures are very similar and are presented as yellow spheres. The substrate β -Asp-His is presented with gold bonds. The image was drawn with the program WebLab viewer Pro.

3.3. X-ray structures of the E77Q and Y137F mutant proteins

The three dimensional X-ray structures of the E77Q and Y137F mutant proteins were determined to a resolution of 1.95 Å with *R*-factors of 18.0 and 18.5%, respectively². The mutation of these two residues within the active site of IAD did not affect the relative occupancies of the zinc ions in the binuclear metal center. The overall molecular fold of the mutant proteins is identical to that of the wild-type IAD. The electron density of Lys-162 in both of the subunits is consistent with the carboxylation of the side-chain ϵ -amino group to a carbamate functional group. In the previously determined structure of the D285N mutant complexed with the substrate β -Asp-His, the side-chain carboxylate of Glu-77 appears to ion pair to the α -amino group of the β -Asp-His substrate [4]. Interestingly, the orientation of Gln-77 in the E77Q mutant is similar to that obtained for the crystal structures of the wild-type IAD complexed with the product aspartate and the D285N mutant complexed to β -Asp-His (Fig. 3) rather than of the apo-form of IAD. However, the γ -carbonyl oxygen of Gln-77 in the E77Q mutant remains virtually in the same position as one of the oxygens of the γ -carboxylate of Glu-77.

The superposition of the active site residues for the unliganded form of IAD and the Y137F mutant is presented in Fig. 4. In the structure of the wild-type enzyme the Oⁿ

² X-ray coordinates have been deposited in the Protein Data Bank (Accession Nos. 2AQO and 2AQV).

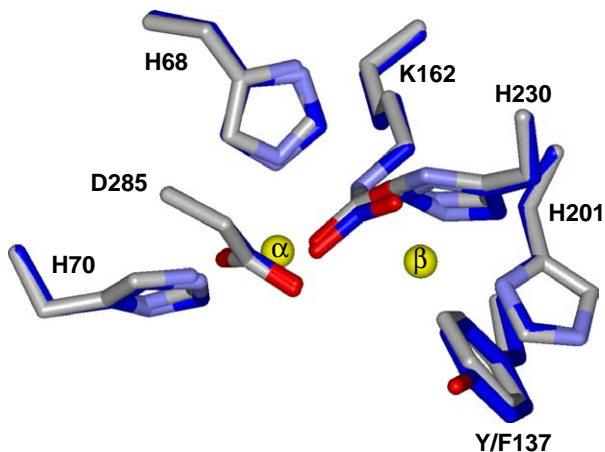


Fig. 4. Superposition of the wild-type IAD (PDB: 1ONW) and the Y137F mutant (PDB: 2AQV). The side chains corresponding to the wild-type enzyme are depicted in the dark blue bonds while those of the Y137F mutant protein are displayed in light blue. The positions of the zinc ions both structures are essentially the same and are indicated by yellow spheres. The solvent molecule that bridges the binuclear metal center is drawn as a red sphere. The image was created with the program WebLab Viewer Pro.

for the side-chain of Tyr-137 is situated 3.4 Å from the β -metal and 2.4 Å from the carbonyl oxygen of the scissile peptide bond of the substrate. The removal of the phenolic hydroxyl from the side-chain of Tyr-137 did not result in any significant perturbation of the phenyl ring relative to the corresponding side-chain within the active site of the wild-type enzyme.

4. Discussion

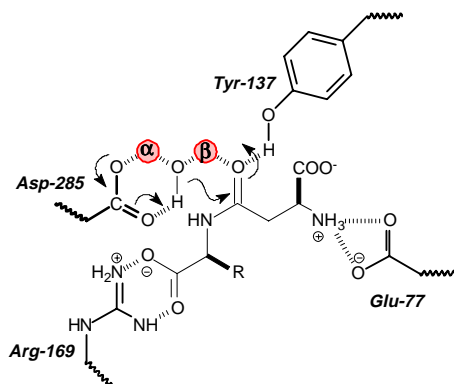
Isoaspartyl dipeptidase is a member of the amidohydrolase superfamily [5,6]. IAD catalyzes the hydrolysis of β -aspartyl dipeptides with a variety of side chains at the C-terminus. These variations include amino acid residues that are hydrophobic, aromatic, or hydrophilic. The binuclear metal center of IAD is similar to that found for phosphotriesterase [14], dihydroorotase [15], and urease [16]. The reaction mechanism for IAD proposed in Scheme 2 postulates the activation of the solvent molecule between the two metals via proton transfer to the carboxylate group of Asp-285. The pH-rate profiles for the wild-type IAD display a significant decrease in catalytic activity at pH values lower than 6 and higher than 9. The loss of catalytic activity at low pH suggests the protonation of a single group with a pK_a of ~ 6 . The kinetic pK_a , obtained from the pH-rate profiles of metal-substituted variants of IAD, was found to be dependent on the specific metal ion bound to the active site [4]. The loss of the catalytic activity at low pH is consistent with the protonation of the bridging hydroxide [4]. In contrast, the kinetic pK_a for the group that must be protonated for catalytic activity was independent of the specific metal ion bound to the active site. The decrease in the catalytic activity at high pH was proposed to be caused by the deprotonation of the α -amino group of the aspartate moiety of the substrate [4].

Amino acid sequence alignments and the three dimensional X-ray structures of IAD have identified two highly conserved residues within the active site that are not directly

a part of the binuclear metal center. However, the precise functions of Glu-77 and Tyr-137 in the catalytic reaction mechanism are not known. When Tyr-137 is mutated to either alanine or phenylalanine the catalytic activity is reduced by approximately three orders of magnitude. The pH-rate profiles for the Y137F mutants are similar to the wild-type enzyme in that activity is lost as the pH is lowered below ~ 6 or elevated above ~ 9 . These results suggest that ionization of this residue is unlikely to be responsible for the loss of catalytic activity observed in the pH-rate profiles of the wild-type enzyme. However, the significant drop in catalytic activity for the Y137F mutant does suggest a critical role for the phenolic hydroxyl of Tyr-137. The X-ray structure of the Y137F mutant reported here shows that the aromatic ring of the phenylalanine is oriented in precisely the same way as the aromatic ring of the tyrosine found in the structure of the wild-type enzyme. This observation rules out the possibility of a conformational difference between the mutant and the wild-type enzyme as the root cause for the diminution of catalytic activity.

In the structure of the inactive D285N mutant bound with the substrate β -Asp-His the phenolic oxygen of Y137 is 2.4 Å away from the carbonyl oxygen of the scissile peptide bond. This distance is consistent with a hydrogen bond from the tyrosine to the tetrahedral intermediate during hydrolysis of the peptide bond. This feature within the active site would serve to augment the stabilization of the tetrahedral intermediate by the β -metal ion. However, residues with similar function have not been detected within the active sites of phosphotriesterase [14], dihydroorotase [15], or urease [16].

When the side-chain carboxylate of Glu-77 is mutated to either aspartate or glutamine the catalytic activity is reduced by about five orders of magnitude. Unfortunately, the dramatic loss in catalytic activity precluded an accurate assessment of the overall effects on the pH-rate profiles for the mutant enzyme. Nevertheless, the three dimensional X-ray structure of the E77Q mutant demonstrates that the net loss in catalytic activity is not due to any apparent conformational differences between the wild-type and mutant enzyme. In the X-ray structure of the D285N protein, determined in the presence of the bound substrate β -Asp-His, the side-chain carboxylate of Glu-77 is ion paired with the free α -amino group of the substrate. Therefore, the most likely function of Glu-77 is to help orient the substrate within the active site. This ion pair is critical for catalytic activity since the removal of the free amino group in dipeptide substrates results in the loss of catalytic activity and the ability to function as an inhibitor [4]. The mutation of Glu-77 results in



Scheme 3.

relatively minor effects on the K_m for the substrate β -Asp-Leu. The substantially larger effects on k_{cat} must therefore reflect a coupling of ion pair formation with catalytic turnover.

In this investigation, we have explored the role of two highly conserved residues in the active site of isoaspartyl dipeptidase. The side-chain carboxylate of Glu-77 is critical for catalytic activity through an ion pair interaction with the free α -amino group of dipeptide substrates. The phenolic hydroxyl of Tyr-137 serves as a Lewis acid catalyst via stabilization of the tetrahedral adduct formed upon nucleophilic attack by the bridging hydroxide within the binuclear metal center. The remaining critical residue is the highly conserved Arg-169 that makes an ion pair with the terminal carboxylate of the substrate. These molecular interactions are summarized in [Scheme 3](#).

Acknowledgments

This work was supported in part by NIH Grants GM-33894. R.M.-A. was supported as a trainee of the Chemistry-Biology Interface Training Program (T32GM 008523).

References

- [1] J.D. Gary, S. Clarke, *J. Biol. Chem.* 270 (1995) 4076–4087.
- [2] J.D. Gary, S. Clarke, *Handbook of Proteolytic Enzymes*, Academic Press, New York, 1998, 1461–1465.
- [3] E.E. Haley, *J. Biol. Chem.* 243 (1968) 5748–5752.
- [4] R. Martí-Arbona, V. Fresquet, J.B. Thoden, M.L. Davis, H.M. Holden, F.M. Raushel, *Biochemistry* 44 (2005) 7115–7124.
- [5] C.M. Seibert, F.M. Raushel, *Biochemistry* 44 (2005) 6383–6391.
- [6] L. Holm, C. Sander, *Proteins: Struct. Funct. Genet.* 28 (1997) 72–82.
- [7] D. Jozic, J.T. Kaiser, R. Huber, W. Bode, K. Maskos, *J. Mol. Biol.* 332 (2003) 243–256.
- [8] J.B. Thoden, R. Martí-Arbona, F.M. Raushel, H.M. Holden, *Biochemistry* 42 (2003) 4874–4882.
- [9] M. Hejazi, K. Piotukh, J. Mattow, R. Deutzmann, R. Volkmer-Engert, W. Lockau, *Biochem. J.* 364 (2002) 129–136.
- [10] W.W. Cleland, *Methods Enzymol.* 63 (1979) 103–138.
- [11] W. Kabsch, *J. Appl. Crystallogr.* 21 (1988) 67–71.
- [12] W. Kabsch, *J. Appl. Crystallogr.* 21 (1988) 916–924.
- [13] D.E. Tronrud, L.F. Ten Eyck, B.W. Matthews, *Acta Crystallogr. A* 43 (1987) 489–501.
- [14] M. Benning, H. Shim, F. Raushel, H. Holden, *Biochemistry* 40 (2001) 2712–2722.
- [15] J.B. Thoden, G.N. Phillips Jr., T.M. Neal, F.M. Raushel, H.M. Holden, *Biochemistry* 40 (2001) 6989–6997.
- [16] E. Jabri, M.B. Carr, R.P. Hausinger, P.A. Karplus, *Science* 268 (1995) 998–1004.